Journal of Crohn's and Colitis, 2024, **18**, 121–133
https://doi.org/10.1093/ecco-jcc/jjad122
Advance access publication 11 August 2023
Original Article

Myenteric Plexus Immune Cell Infiltrations and Neurotransmitter Expression in Crohn's Disease and Ulcerative Colitis

Jakob J. Wiese,[a] Subhakankha Manna,[a] Anja A. Kühl,[b] Alberto Fascì,[a] Sefer Elezkurtaj,[c] Elena Sonnenberg,[a] Marvin Bubeck,[d] Raja Atreya,[d] Christoph Becker,[d] Benjamin Weixler,[e] Britta Siegmund,[a] Jay V. Patankar,[d] Magdalena S. Prüß,[a,f] Michael Schumann[a,f,*]

[a]Medizinische Klinik m. S. Gastroenterologie, Infektiologie und Rheumatologie, Charité – Universitätsmedizin Berlin, Freie Universität Berlin and Humboldt-Universität zu Berlin, Berlin, Germany
[b]Charité – Universitätsmedizin Berlin, Freie Universität Berlin and Humboldt-Universität zu Berlin, iPATH.Berlin, Berlin, Germany
[c]Institute of Pathology, Charité – Universitätsmedizin Berlin, Freie Universität Berlin, Humboldt-Universität zu Berlin, Berlin, Germany
[d]Department of Internal Medicine 1, University Hospital Erlangen, Faculty of Medicine, Erlangen, Germany
[e]Klinik für Allgemein- und Viszeralchirurgie, Charité – Universitätsmedizin Berlin, Freie Universität Berlin, Humboldt-Universität zu Berlin, Berlin Institute of Health, Berlin, Germany
[f]Berlin Institute of Health at Charité – Universitätsmedizin, – Berlin, BIH Biomedical Innovation Academy, BIH, Charité Clinician Scientist Program, 10178 Berlin, Germany

[*]Corresponding author: Dr Michael Schumann, Hindenburgdamm 30, 12200 Berlin, Germany. Tel.: +49 [0] 30 450 514 536; Fax: +49 [0] 30 450 514990; Email: michael.schumann@charite.de

Abstract

Background and Aims: Pain is a cardinal symptom in inflammatory bowel disease [IBD]. An important structure in the transduction of pain signalling is the myenteric plexus [MP]. Nevertheless, IBD-associated infiltration of the MP by immune cells lacks in-depth characterisation. Herein, we decipher intra- and periganglionic immune cell infiltrations in Crohn´s disease [CD] and ulcerative colitis [UC] and provide a comparison with murine models of colitis.

Methods: Full wall specimens of surgical colon resections served to examine immune cell populations by either conventional immunohistochemistry or immunofluorescence followed by either bright field or confocal microscopy. Results were compared with equivalent examinations in various murine models of intestinal inflammation.

Results: Whereas the MP morphology was not significantly altered in IBD, we identified intraganglionic IBD-specific B cell- and monocyte-dominant cell infiltrations in CD. In contrast, UC-MPs were infiltrated by $CD8^+$ T cells and revealed a higher extent of ganglionic cell apoptosis. With regard to the murine models of intestinal inflammation, the chronic dextran sulphate sodium [DSS]-induced colitis model reflected CD [and to a lesser extent UC] best, as it also showed increased monocytic infiltration as well as a modest B cell and $CD8^+$ T cell infiltration.

Conclusions: In CD, MPs were infiltrated by B cells and monocytes. In UC, mostly $CD8^+$ cytotoxic T cells were found. The chronic DSS-induced colitis in the mouse model reflected best the MP-immune cell infiltrations representative for IBD.

Key Words: Enteric nervous system; inflammatory bowel disease; IBD; visceral pain; abdominal pain; immune cell infiltration; myenteric plexus; submucosal plexus

1. Introduction

In inflammatory bowel disease [IBD], a defective intestinal mucosal barrier causes an immune reaction to the commensal flora resident to the intestinal lumen. As a consequence, intestinal mucosal and submucosal tissues are infiltrated by distinct populations of immune cells in a disease-specific pattern, resulting in a transmural [Crohn´s disease, CD] or mostly mucosal [ulcerative colitis, UC] type of inflammatory infiltrate.[1,2] By nature, this involves the local structures of the enteric nervous system [ENS], namely the myenteric and submucous plexus [MP and SMP], as well as the neurite extensions of plexus gangliocytes. These plexuses are of utmost importance as they are the signal-transducing structures for pain signals that are elicited in the context of chronic inflammation.[3] However, studies that focus on the interaction of intestinal mucosal immune cells, via direct physical interaction or through secreted cytokines, with structures of the ENS, are scarce.[4,5]

MP and SMP contain a diverse population of enteric neurons fulfilling a range of functions, including the action of motor, vasodilator, and secretomotor neurons. Equally important, neuronal cells transduce afferent signals, which includes pain signals.[4,5] Specifically, intrinsic primary afferent neurons [IPANs], making up 10–30 % of neuronal cells in both plexuses, and extrinsic primary afferent neurons [ExPANs], with their cell bodies in dorsal root ganglia and their processes extending to the mucosa and to MPs, were shown to contribute

to transmission of pain/visceral hypersensitivity signals from the intestinal wall to the central nervous system [CNS].[6,7] In the murine model of dextran sulphate sodium [DSS]-induced colitis, mimicking the mucosal inflammation in UC, the role of ExPANs in visceral pain perception was investigated. By an optogenetic inhibition of colonic ExPANs, colorectal distension as a noxious stimulus of the visceromotor response was found to be significantly reduced.[8,9] In this regard, projections of myenteric neurons to the mucosa were identified in the intestine of guinea pigs, uncovering the complex network in intestinal pain perception.[10]

Various studies revealed that interactions between afferent ENS fibres and the mucosal immune system, as found in neurogenic inflammation, are part of the immune-pathogenesis of IBDs.[11] Interestingly, the initial discovery of neurogenic inflammation was closely linked [i] to the establishment of the concept of antidromic signalling, as inflammation was triggered by central stimulation of afferent neuronal projections, and [ii] to the identification of peptide neurotransmitters having strong vasodilatory and cell permeability-enhancing properties including substance P [SP], calcitonin gene-related peptide [CGRP], and vasoactive intestinal peptide [VIP].[12,13] As such these neurotransmitters, along with other tachykinins such as neurokinin A and B, are known to be expressed by afferent IPANs as well as ExPANs.[14,15] Aside from allowing diapedesis of immune cells into the lamina propria of the gut wall and activation of effector immune cells, neuropeptides contribute to barrier dysfunction of intestinal epithelial cells and thus have decisive roles in various steps of IBD development.[16–18]

Regarding the integrity of the ENS in IBD, previous findings described various morphological alterations under conditions of inflammation, such as MP ganglion cell hypertrophy, hyperplasia, and axonal necrosis.[19–21] Furthermore, changes in neurotransmitter expression were found in CD, which included increased levels of 5-hydroxytryptamine, neuropeptide Y, vasoactive intestinal polypeptide, and pituitary adenylate cyclase-activating peptide in CD-MP.[22,23] Moreover, a higher number of interstitial cells of Cajal as well as enteroglial cells were detected in CD compared with controls, whereas only increases in enteroglia were found in UC-MP.[24]

However, the composition of immune cells infiltrating the MP in the gut of IBD patients is unclear. Importantly, the interaction of immune cells and neurons in the intestinal wall is described to modulate transmission of pain signals as well as regulation of intestinal motility.[25–28] Thus we determined MP-infiltrating lymphocyte and monocyte subsets, spatially resolved the interactions of distinct immune cells, and analysed the associated neurotransmitter expression and extent of gangliocyte cell death. Importantly, findings in IBD were compared with respective findings in various murine models of intestinal inflammation to prospectively facilitate the selection of an appropriate murine model of intestinal inflammation.

2. Methods

2.1. Study participants

The Ethics Committee of the Charité – Universitätsmedizin Berlin, Germany, approved the study [protocol number: EA2/118/19, accepted on Aug 8, 2019]. All patients included in the study received surgery at the Charité. The paraffin blocks including surgical specimen were requested from the biobank ZeBanC of the Charité. Inclusion criteria were known diagnosis of IBD for >6 months, colon-involving surgery for IBD, or—for the control group—surgery for non-inflammatory reasons [ie, colon resection for colon neoplasms or colon ischaemia]. For inclusion, age was at least 18 years. In the control cases, unaffected colon of the resection borders was used [Table 1, Supplementary Table S1]. Disease activity at the time of surgery [Crohn´s: Harvey–Bradshaw Index, UC: partial Mayo score, ie, Mayo excluding endoscopic scoring] was extracted from the IBD database of the Charité IBD clinic.

2.2. Immunohistochemistry

Immunohistochemistry [IHC] was performed on 2-µm sections of formalin-fixed, paraffin-embedded tissue [FFPE] according to a standard protocol using the ABC-AP Kit, Alkaline Phosphatase [Universal] [VECTASTAIN®, identifier: AK-5200, Vector labs, USA]. Briefly, after retrieval, sections were exposed to the primary antibody diluted in Dako REAL diluent [S202230-2, Agilent Technologies, Waldbronn,

Table 1. Baseline characteristics of study participants.

	Control	Crohn´s disease	Ulcerative colitis
n	10	9	12
Age in years (median [95%–CI])	76 [71–80]	35 [26–44][1]	31 [22–40][2]
Male/female	7/3	4/5	2/10
Resected/ analysed tissue	Colon	Colon	Colon
Type of surgery	Resection of colorectal [*n* = 7], and rectal [*n* = 1] carcinoma, Colonic ischaemia [*n* = 2]	Ileocaecal res. [*n* = 7], ileoascendostomy [*n* = 1], colectomy [*n* = 1]	Colectomy [*n* = 12]
Activity score [HBI score]	NA	9.3 ± 2.6	NA
Activity score [Mayo score]	NA	NA	5.3 ± 0.6

[1]Comparison of age in years (Mann-Whitney-U-Test) for control patients and Crohn's disease patients, p<0.0001.
[2]Comparison of age in years (Mann-Whitney-U-Test) for control patients and ulcerative colitis patients, p<0.0001.
res., resection; HBI, Harvey–Bradshaw Index; NA, not available.

Germany] for 15 min at room temerature [RT], followed by incubation with the biotinylated secondary antibody [30 min, RT] and an incubation with the Vectastain ABC-AP reagent. After a TBS wash, a 5-min exposure to the Vector Blue alkaline phosphatase substrate was done and followed by Tris-buffered saline [TBS] wash. A second retrieval was performed, followed by another primary antibody incubation including all steps described above. The sections were exposed to the ImPACT Vector Red alkaline phosphatase substrate solution for 1-5 min, washed with deionized water and finally haematoxylin-counterstained. Dilutions and antigen-retrieval strategies for antibodies are listed in Supplementary Table S2. Imaging was done using an Axio observer Z1, which was connected to an Axiocam 506 colour [both Carl Zeiss, Jena, Germany].

2.3. Quantification strategy for ganglion morphology and various cell populations

Size [area in μm^2] and interganglionic distance [in µm] of MPs were analysed with the software FIJI. The counting of immune cells infiltrating the ganglia of the MP and immune cells located within the surrounding area was performed as depicted in Figure 1. The cells next to PGP9.5$^+$ cells were defined as intraganglionic cells, whereas the cells in a defined area of 100 µm around the ganglia as periganglionic cells. Both were quantified per area, ie, number of cells per mm^2. For each control or IBD patient, five myenteric ganglia revealing the highest infiltration per area were analysed.

2.4. Immunofluorescence and confocal laser scanning microscopy

The antigen retrieval of the FFPE tissue was performed as described in the paragraph Immunohistochemistry. Immunofluorescence [IF] staining of MP cells and mucosal immune cells was performed using the following primary antibodies: anti-CD8 [1:100; clone: 4SM15; Agilent Technologies, CA, USA], anti-CD68 [1:100; clone: PG-M1; GeneTex, CA, USA], anti-CD163 [1:100; clone: 10D6; Novocastra, Germany], and anti-βIII-tubulin [1:100; clone: TUJ1; biotinylated antibody; Novocastra, Germany]. As secondary antibodies, AlexaFluor594 goat anti-mouse IgG [1:500; Thermo Fisher Scientific, MA, USA] was used. The biotinylated βIII-tubulin antibody was detected using Strepavidin-DyLight488 [1:100; Thermo Fisher Scientific, MA, USA]. DAPI [4′,6-diamidin-2-phenylindol] was used for the staining of nuclei [1:3000]. Incubation conditions for all antibodies were 1 h at 37°C. Imaging was done using the confocal laser scanning system LSM780 [Carl Zeiss, Jena, Germany] as previously described.[29,30]

2.5. RNA isolation and cDNA synthesis

Up to six 10-µm sections were cut from archived FFPE blocks and placed in sterile 1.5-mL centrifuge tubes. Total RNA was isolated using RNeasy FFPE Kit [Qiagen Cat# 73504] following manufacturer's protocol. RNA quantity was measured using NanoDrop 1000. 1 µg of total RNA was reverse-transcribed using High-Capacity cDNA Reverse Transcription Kit [Thermo Scientific, Cat# 4368814].

2.6. Quantitative polymerase chain reactions

Real-time quantitative polymerase chain reactions [qPCRs] were performed in 384-well plates using TaqMan Universal PCR Master Mix [Thermo Scientific Cat# 4304437] and the following TaqMan gene expression assays: TAC1 Hs00243227_m1, TACR1 Hs00185530_m1, CALCA Hs01100741_m1, RAMP1 Hs00195288_m1, CALCRL Hs00907738_m1, TRPV1 Hs00218912_m1, TRPV4 Hs01099348_m1, 18s Hs99999901_s1 and β-Actin Hs01060665_g1. Fluorescence was detected using QuantStudio 5 Real-Time PCR system [Thermo Scientific]. Fold changes were calculated with the ΔΔCT method using 18s and β-Actin as housekeeping genes.

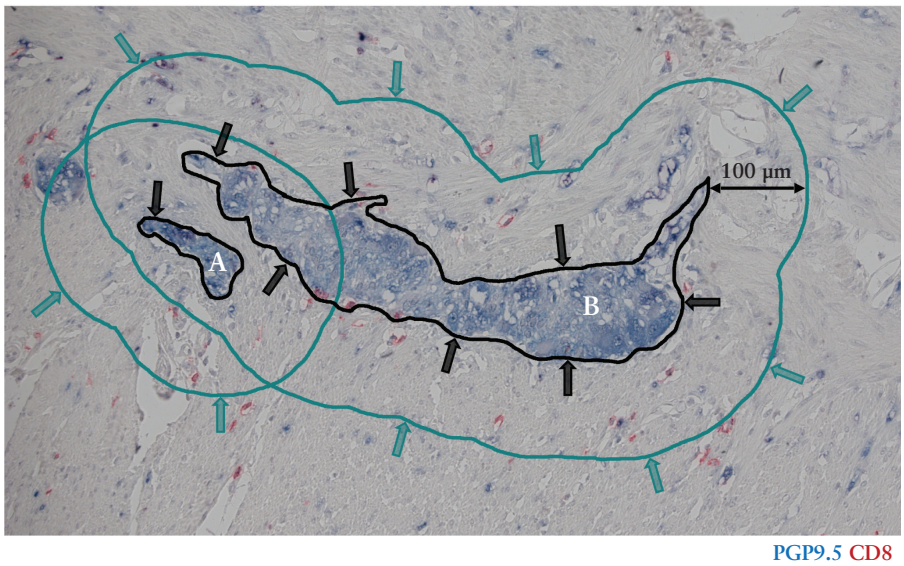

Figure 1. Immunohistochemistry [IHC] staining of a myenteric plexus [MP] [blue: PGP9.5] with intra- and periganglionic infiltration by CD8$^+$ cytotoxic T cells (red, 100x magnification, prepared from ulcerative colitis [UC] colectomy tissue). Immune cells are identified either in the intraganglionic areas [black arrows; A and B] or in the surrounding area [radius 100 µm, periganglionic cells, green arrows]. Cell cores are stained with haematoxylin; scale bar, 100 µm.

2.7. Murine models of colitis, intestinal sections, and immunostaining

The protocols for murine models of intestinal inflammation were conducted as previously described.[31,32] Control mice were C57BL/6-mice at the age of 6 to 16 weeks. Inflammatory activity was determined by the established murine colitis histopathology score by Erben *et al.*[33]

For the acute DSS-induced colitis model, C57BL/6 mice were exposed to 2% DSS salt dissolved in drinking water [MW_{DSS} 36-50 kDa; identifier: 0216011090, MP Biomedicals, Germany] for 8 consecutive days. After this induction phase, mice were sacrificed and analysed.[31]

In the chronic DSS-induced colitis, during the first induction phase of 8 days, 1.5% DSS was added to the drinking water, followed by 14 days of regular drinking water. This procedure was repeated for two more cycles including induction phases in which 1.5% DSS was provided in the drinking water. The mice were sacrificed and analysed at Day 47.[31]

For transfer colitis [T cell-mediated colitis], naïve $CD4^+CD45RB^{high}$ T cells were transferred from C57BL/6 WT mice to immunodeficient *Rag*$^{-/-}$ mice. T cell transfer animals developed severe disease manifestations ie, weight loss and diarrhoea, and were sacrificed and analysed after 7 weeks.[32]

Chronic 2,4,6-trinitrobenzenesulphonic acid [TNBS] colitis was induced in C57BL/6 mice by an intrarectal administration of a TNBS/ethanol solution. One week before the first injection, mice were presensitised by application of 150 µl of 1% [wt/vol] TNBS to the back of the mouse. On Day 1, 100 µl 2.5% [wt/vol] weas administered as enema using a catheter. After 1 week, 100 µl of 0.75% [wt/vol] TNBS solution was injected; after 2 weeks, 100 µl of 1.5% [wt/vol] TNBS solution and, after 3 weeks, 100 µl of 2.5% [wt/vol] TNBS solution; followed by three further injections of 100 µl of 2.5% [wt/vol] TNBS solution at weekly intervals. The mice were sacrificed 7 weeks after the first TNBS injection.[31]

Casp8$^{\Delta IEC}$-mice were generated by introduction of a conditional intestinal-epithelial caspase 8-knock-out as described by Stolzer *et al.*[34]; 6–12 week-old mice were sacrificed and analysed.

Sections were 2 µm in thickness. The staining procedure followed exactly the protocol used for the human samples described above. All antibodies used for immunostaining of murine tissues are listed in Table S2.

2.8. Statistics

Statistical analysis was performed using the GraphPad Prism software [version 9, by GraphPad, CA, USA]. For comparisons of immune cell infiltration, neurotransmitter expression and size differences of myenteric ganglia, the Mann–Whitney U test was applied. Since numerous immune cell populations were analysed in parallel, calculated significance levels were corrected for multiple testing [Bonferroni correction]. Data are presented as mean and standard error of the mean [SEM]. Correlations of age and respective immune markers and neurotransmitter levels were determined using linear regression. In the murine colitis models, immune cell infiltration and apoptosis data were analysed by one-way analysis of variance [ANOVA]. A p-value <0.05 was considered to be statistically significant in all statistical tests applied.

3. Results

3.1. Characterisation of study participants

In total, 31 patients either suffering from IBD [n = 21] or non-IBD patients [n = 10] were included. Patient characteristics are summarised in Table 1 and Supplementary Table S1. The type of surgical resections performed comprised: [1] CD: ileocaecal resections [n = 7], ileoascendostomy [n = 1], and a colectomy [n = 1]; [2] UC: colectomies [n = 12]; and [3] non-IBD patients ['controls']: partial colectomies for colon carcinoma [n = 7], rectal carcinoma [n = 1], and ischaemia [n = 2]. For analysis of MP, only colon wall tissue was used. From control patients, vital and non-tumorous tissue of the resection borders was analysed. IBD activity, as analysed by Harvey–Bradshaw index [HBI] for CD [mean HBI 9.3 ± 2.6] or the partial Mayo score for UC [mean partial Mayo score 5.3 ± 0.6], suggested a moderate disease activity.

3.2. Size and density of MP ganglia is not altered in IBD

After immunostaining the full-wall colonic MP ganglia for PGP9.5, ganglia of all IBD and of control patients were compared regarding ganglion size and density, to identify if MP morphology is influenced by IBD. The number of analysed ganglia added up to: CD: n = 315, UC: n = 420, and controls: n = 350. Interestingly, surface areas of analysed MP ganglia were not significantly different for patient groups [CD: $1.1 \times 10^4 \pm 2.0 \times 10^3$ µm², UC: $1.3 \times 10^4 \pm 2.1 \times 10^3$ µm², controls: $1.3 \times 10^4 \pm 1.9 \times 10^3$ µm² Supplementary Figure S1]. Also, the average interganglionar distance [ie, the distance between two MPs] as a measure of MP density was not significantly different for the two IBD groups versus the controls [interganglionar distance for CD 79 ± 10 µm, for UC 128 ± 17 µm, and for controls 107 ± 8 µm].

3.3. IBD-specific infiltration of MP by T and B lymphocytes

MP-infiltrating T and B cell populations, as analysed by IHC, revealed an IBD-specific pattern [Figure 2]. In CD, MPs were infiltrated by $CD3^+$ T cells [7.2-fold increase in comparison with control MPs, p = 0.0427]. Figure 3 shows IHC of a control patient [A] and a CD patient [A']. Intraganglionic numbers $CD4^+$ and $Foxp3^+$ T cells were not altered. However, further staining revealed an infiltration by $CD8^+$ T cells [increased by 11.1-fold as compared with controls, p = 0.0063] and $CD20^+$ B cells [control patients: 0 cells/10.000 µm², CD: 0.89 ± 0.32 cells/10.000 µm², p = 0.02; Figure 2 and 3B, B"]. Periganglionic immune cell infiltrations in CD revealed a similar pattern: $CD3^+$ T cells: 9.1-fold significant increase compared with control MPs, p = 0.01; $CD4^+$ T cells: 6-fold significant increase, p = 0.04; $CD8^+$ T cells: 36-fold significant increase, p = 0.001; $Foxp3^+$ T cells: 0 cells/10.000 µm², CD: 0.24 ± 0.06 cells/10.000 µm², p = 0.001; $CD20^+$ B cells: control patients: 0 cells/10.000 µm², CD: 0.83 ± 0.29 cells/10.000 µm², p = 0.001; Figure S2A and B.

In UC, the numbers of intraganglionic T and B lymphocytes were not significantly altered. However, $CD8^+$ periganglionic T cells were increased by 4.3-fold [p = 0.0497, Supplementary Figure S2A]. In Figure 3 immunohistochemistry of a control patient [A] and an UC patient [A"] reveal differences in intra- and periganglionic infiltration by $CD8^+$ T cells of the myenteric ganglia. Infiltration of MPs by B cells was unaltered in UC [Figures 2B, 3B" and Supplementary Figure 2B].

Since the control patients included in the study were older than the patients of the disease groups [Table 1], correlation between the age and counts of infiltrations were analysed for all patients. This analysis represents the impact of the age of patients on the infiltration of myenteric ganglia by immune

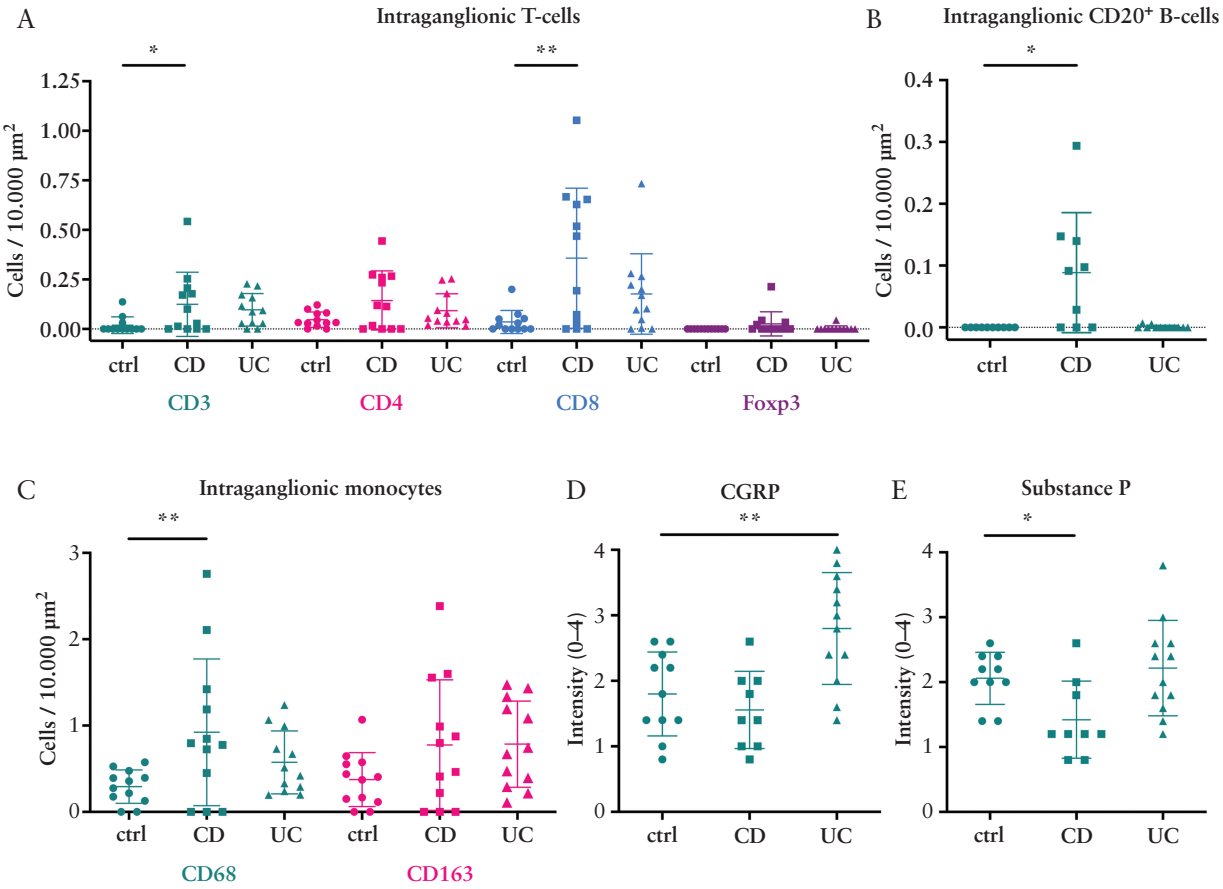

Figure 2. Intraganglionic MP-immune cell infiltrations in IBD. Conventional immunohistochemistry followed by quantification by bright field microscopy. [A] T cell populations: CD3⁺, CD4⁺, CD8⁺, and Foxp3⁺. [B] Bcell populations: CD20⁺. [C] Monocyte populations: CD68⁺, CD163⁺. [D] Expression of the neurotransmitters CGRP and [E] SP. N[CD] = 9, N[UC] = 12, N[ctrl] = 10; ctrl, control. Significance levels were determined by testing with Mann–Whitney U test, followed by a Bonferroni correction for multiple testing; *p <0.05; **p <0.01. IBD, inflammatory bowel disease; MP, myenteric plexus.

cells. Cell counts for control and diseased patients were analysed as one group. No significant correlation was found for age and intra- or periganglionic CD3⁺, CD4⁺, CD8⁺, Foxp3⁺, or CD20⁺ cells [Supplementary Figure S3A–D and G].

Therefore, the lymphocytic infiltrate of MP in IBD comprises CD3⁺, CD8⁺, and CD20⁺ cells in CD. Contrary to that, UC-MP reveal a periganglionic infiltration by CD8⁺ cells. An illustration of the scatter associated with individual immunohisto-readings, which facilitates assessing the validity of the data, is added as Supplementary Figure. 9.

3.4. Monocytic infiltrations of MP in IBD

We performed immunohistochemical staining of CD68⁺ and CD163⁺ cells to quantify the numbers of monocytes in MPs. For CD, the numbers of intraganglionic CD68⁺ monocytes were significantly increased by 3.5-fold [p = 0.001]. However, for CD163⁺ monocytes no difference was observed [Figures 2C and 4C, G]. Interestingly, these infiltrations were solely intraganglionic, since neither periganglionic CD68⁺ nor CD163⁺ cells were found to be altered. In UC, no differences in MP-infiltrating monocytes were found when compared with controls. There was a significant negative correlation for intraganglionic CD163⁺ monocytes with age [p = 0.04], whereas all other monocyte markers analysed showed no relevant correlations [ie, periganglionic CD68⁺ or CD163⁺ cells, intraganglionic CD68⁺ cells, Supplementary Figure S3E and F]. Therefore, significant infiltrations of MPs by monocytes were only found in CD. Since monocytes were shown to be chemotactically attracted by monocyte chemoattractant protein-1 [MIP1] binding to its CC chemokine receptor type-2 [CCR2],[35] we looked for CCR2 expression in the MP CD68-monocyte population [Supplementary Figure 8]. First, we detected CCR2 in a substantial part of the monocytes that infiltrate the MP, which in general complies with our hypothesis. Second, CCR2 was strongly expressed also by βIII-tubulin positive MP cells. Third, the proportion of intraganglionic monocytes expressing CCR2 in UC and CD MPs was reduced by trend, when compared with control.

3.5. Apoptosis of MP cells in IBD

To determine apoptotic cell death within MP ganglia, we immunostained IBD patient and control MP using Annexin V. Since assigning staining results to single cellular structures was impossible, we performed a scoring of myenteric ganglia regarding the extent of apoptosis [scoring from 0 for no apoptotic cells to 4 for a high proportion of apoptotic cells in and directly next to the ganglia; Figure 3C, C', C" and Figure 5]. When determining cell death in CD MPs in total, we did not identify a significant difference compared with control MPs. Nevertheless, we identified a correlation of MP cell death CD-MPs with CD disease activity [Supplementary Figure 4]. By comparison, UC-MPs revealed a 1.6-fold higher extent of apoptosis [UC: 3.1 ± 0.4 units, controls: 1.9 ± 0.4 units, p = 0.035 by chi square test]. Correlating the age with

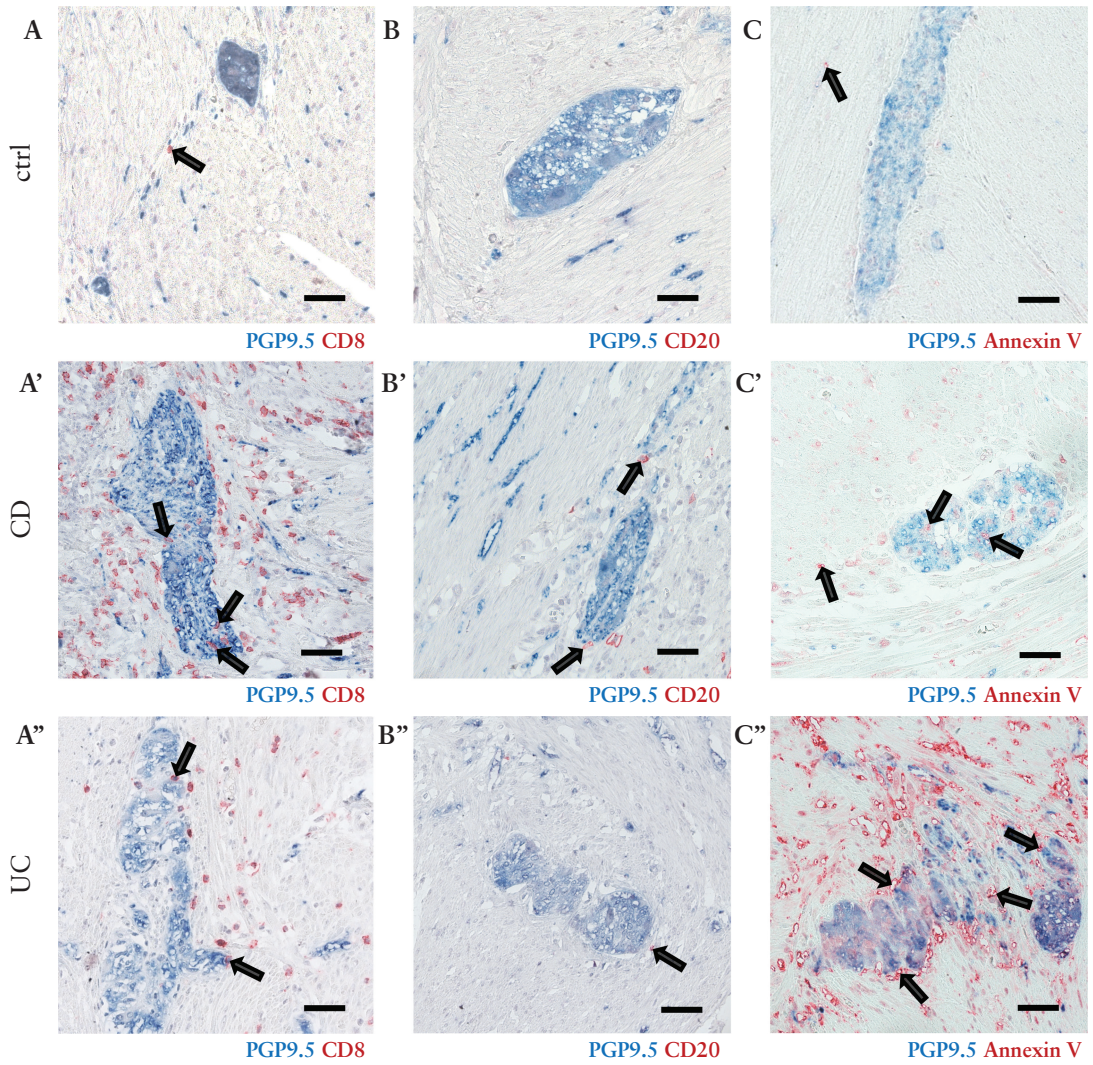

Figure 3. Immune cell infiltrations of MP. MP gangliocytes were stained with PGP9.5 [blue]. [A] CD8 [red] in control, [A'] in CD, and [A"] in UC revealing intra- and periganglionic infiltration by $CD8^+$ cytotoxic T cells, black arrows. [B] CD20 [red] in control, [B'] CD-MP, and [B"] UC-MP, black arrows; 20x objective; scale bar: 40 µm. [C] Annexin V [red] reveals absence of apoptotic cells in controls, whereas [C'] in CD and [C"] in UC apoptotic MP cells are present, black arrows; 40x objective; scale bar, 40 µm. MP, myenteric plexus; CD, Crohn's disease; UC, ulcerative colitis.

annexin V^+ cell scores did not reveal a statistically significant interdependence.

3.6. Protein expression of CGRP, substance P, TRPV1, and TRPV4

Immunostained sections were used to quantify the protein expression of the neurotransmitters CGRP and substance P [SP, for quantifications see Figure 2D, E, and representative staining in Figure 6]. The expression level of CGRP was increased by 1.6-fold in UC-MPs [$p = 0.01$], whereas it reduced by trend in CD-MPs [Figure 2D]. Interestingly, this trend was more distinct when CGRP expression was correlated with the disease activity of the patients [HBI score, Supplementary Figure 4]. Since we had identified infiltrations of MPs by CD8- and CD68-positive cells, we did co-stainings with CGRP, followed by confocal LSM to analyse the differential CD8 and CD68 infiltrations in CGRP-positive and -negative MPs. The CD8 infiltrations in CGRP-positive ganglia were only moderate, which might reflect a reduction of CGRP expression in MPs by infiltrating CD8-positive cells. Interestingly, CD68-positive cells were found to be high in CGRP-positive MPs in UC [Supplementary Figure 6]. SP expression was reduced in the MP of CD patients when compared with controls [0.7-fold, $p = 0.014$], whereas it was unchanged in UC-MPs [Figures 2E, 5C, D, G, H and Figure 6]. Neither for CGRP nor for SP, was a significant correlation of age and expression levels observed [Supplementary Figure S3 H and I].

We also isolated RNA from FFPE sections and performed RT-PCRs to quantify the RNA expression of the neurotransmitters CGRP, SP, and their receptors. Aiming for reproducible RNA expression results from a structure in the tissue section as small as the MPs is difficult, and complicated by the fact that RNA even from fresh FFPE material contains a relevant portion of fragmented RNA. Thus, the data need to be interpreted with caution. In this analysis, we did not identify significant changes in RNA expression of the neurotransmitter [CALCA, TAC1] and neurotransmitter receptor genes [CALCRL, RAMP1, TACR1] in IBD colon sections when compared with control colon sections [Supplementary Figure 5].

Moreover, we performed co-immunostainings to compare the protein expression of the pro-nociceptive cation channels

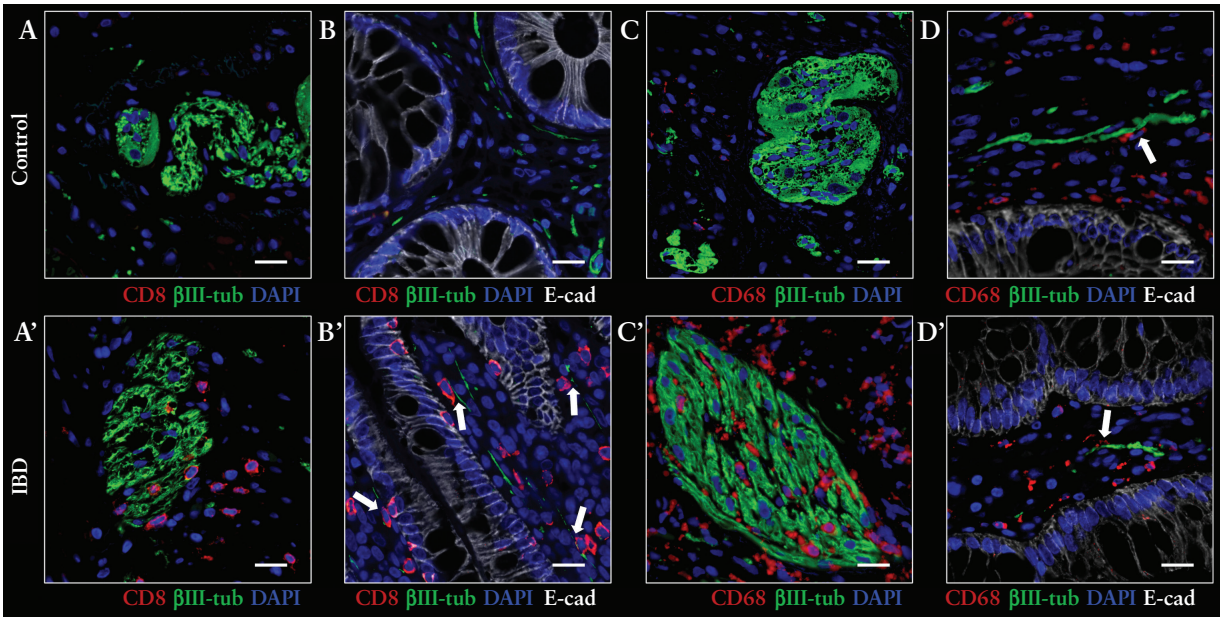

Figure 4. Spatial resolution of immune cells relative to plexus gangliocytes and neurite projections. Immunofluorescence staining followed by laser scanning confocal microscopy [green: PGP9.5]. [A] Lack of CD8⁺ immune cells in control MP. [A'] CD8⁺ cells in MP in UC. [B] Lamina propria infiltrations. Lack of CD8⁺ cells in controls. [B'] CD8⁺ T cells [red] close to βIII-tubulin+ neurites within the lamina propria of UC patients [white arrows]. [C] Lack of CD68⁺ monocytes in control. [C'] Infiltration by CD68⁺ monocytes [red] in a CD patient. [D, D'] Co-localisation of CD68⁺ monocytes [red] and βIII-tubulin⁺ neurites within the lamina propria in a control and a CD-patient, respectively. 40x objective, scale bar, 20 μm. MP, myenteric plexus.

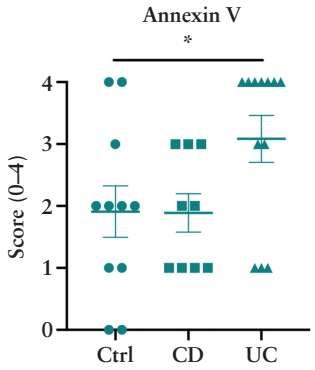

Figure 5. Quantification of MP cell apoptosis in the IBDs. IHC staining was performed using an Annexin Vantibody. The staining intensity in MP cells was scored from 0 [no apoptotic cells], to 4 [high proportion of apoptotic cells] in and directly next to the myenteric ganglia. Scores from 0 to 2 were defined as low-grade infiltration and scores from 3 to 4 as high-grade infiltration. For statistical analysis, low- and high-grade infiltration were compared with chi square test. N[CD] = 9, N[UC] = 12, N[ctrl] = 10; *p <0.05. MP, myenteric plexus; IBD, inflammatory bowel disease; IHC, immunohistochemistry.

transient receptor potential vanilloid-1 and -4 [TRPV1 and -4] in CD and UC MPs, and stratified this along the infiltrations of MPs by either CD8- or CD68-positive cells [Supplementary Figure 7]. TRPV1 protein expression was unchanged in IBD. However, we found a reduced TRPV4 protein expression in CD MPs with a strong CD8 infiltration and an increased TRPV4 protein expression in UC MPs with a high CD8 cell infiltration and—in both IBDs—in MPs with a high CD68 cell infiltration [Supplementary Figure 7A and B]. RNA expression of the TRPV1 and TRPV4 genes was unchanged in the IBDs compared with control [Supplementary Figure 5].

3.7. Close localisation of immune cells and enteric neuronal projections in IBD mucosa

To better understand potential interactions of enteric neurons and immune cells, we applied confocal microscopy to identify βIII-tubulin positive enteric neuronal projections, confirming that not only immune cells infiltrate MPs but also that immune cells also have spatial contact with mucosal neurites. In UC, we identified lamina propria CD8⁺ T cells to be in close proximity to βIII-tubulin⁺ neurites [Figures 4B' and 7A]. Moreover, in CD, CD68⁺ and CD163⁺ monocytes co-localised to βIII-tubulin⁺ mucosal neurites, a co-localisation that was interestingly found also in some controls [Figure 4D, D', and 7B].

3.8. Comparison of IBD-MP infiltrations with murine models of intestinal inflammation

To compare the immune cell infiltrations of colonic myenteric ganglia in IBD patients with the infiltration patterns found in various murine models of colitis, immunostainings of murine colon sections were performed using tissue from T cell transfer colitis, chronic TNBS-induced colitis, and acute and chronic DSS-induced colitis, as well as *Casp8*$^{\Delta IEC}$-colitis [Supplementary Table S5]. Disease activity scoring revealed significantly increased histopathology scores for the respective murine models [Figure 8 and Supplementary Table 6]. Human and murine colitis were compared with each other regarding their MP infiltrations: [i] by monocyte/macrophages, [ii] by B cells, [iii] by T-helper cells, and [iv] by cytotoxic T cells [Figure 8]. Significantly increased percentages of plexus infiltrated by F4/80⁺ cells were found in chronic DSS-induced colitis [p = 0.0001], chronic TNBS-induced colitis [p = 0.004], and in T cell transfer colitis [p = 0.0001]. Moreover, a significant B cell and a modest CD8⁺ T cell infiltration of MPs was found specifically in chronic DSS-induced colitis and only to a lesser extent in acute DSS, TNBS, and transfer colitis. No

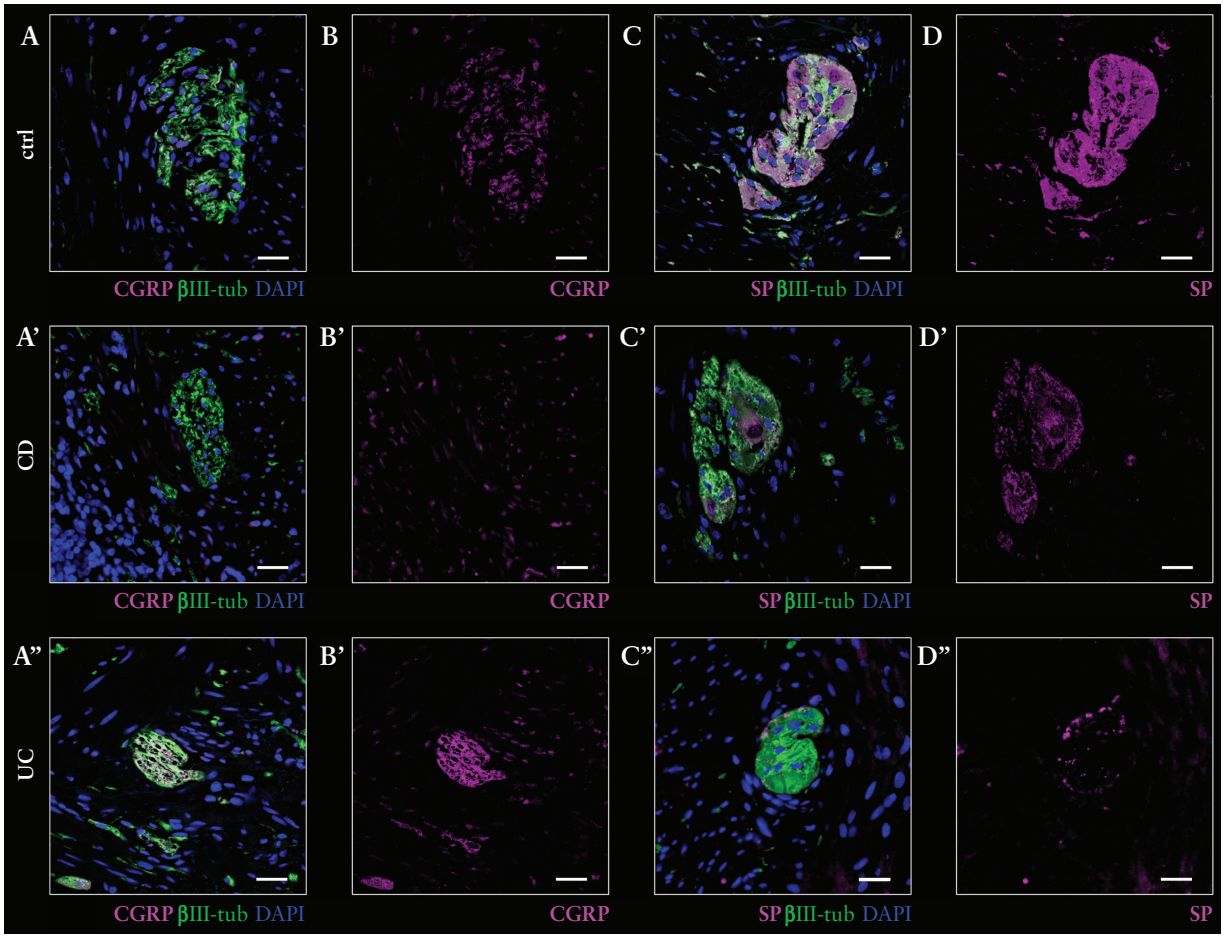

Figure 6. CGRP and SP expression in IBD-MP. [A] Control MP [green, βIII-tubulin⁺ neurites]. [B] Representative CGRP expression [magenta] in the same MP as [A], revealing a low CGRP expression in controls. [A' and B'] Very low CGRP expression in CD-MP. [A" and B"] High myenteric CGRP expression in UC. [C and D] High SP expression [magenta] in controls. [C' and D'] Reduced SP-expression in CD. [C" and D"] Partially very high and low expression of SP in UC-MP. Images were generated with the same microscope settings for control and disease for CGRP and SP, respectively; 40x objective, scale bar, 20 μm.

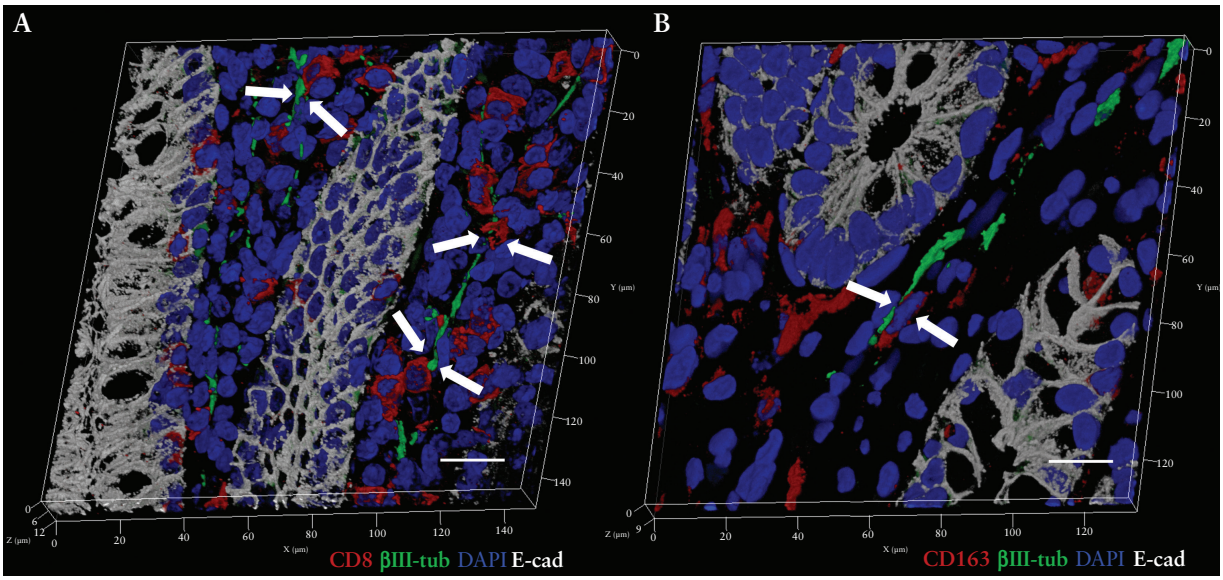

Figure 7: 3D reconstruction of a lamina propria section. 3D-rendered Z-stacks of IF by confocal laser scanning microscopy [ZenBlack, Zeiss, Germany]. [A] Proximity of CD8⁺ cytotoxic T cells [red] and βIII-tubulin⁺ neurites [green] within the lamina propria of a UC patient. [B] CD163⁺ monocyte [red] in the lamina propria directly next to a βIII-tubulin⁺ neurite [green] of a CD patient; 63x objective, scale bar, 20 μm. MP, myenteric plexus; CD, Crohn's disease; UC, ulcerative colitis.

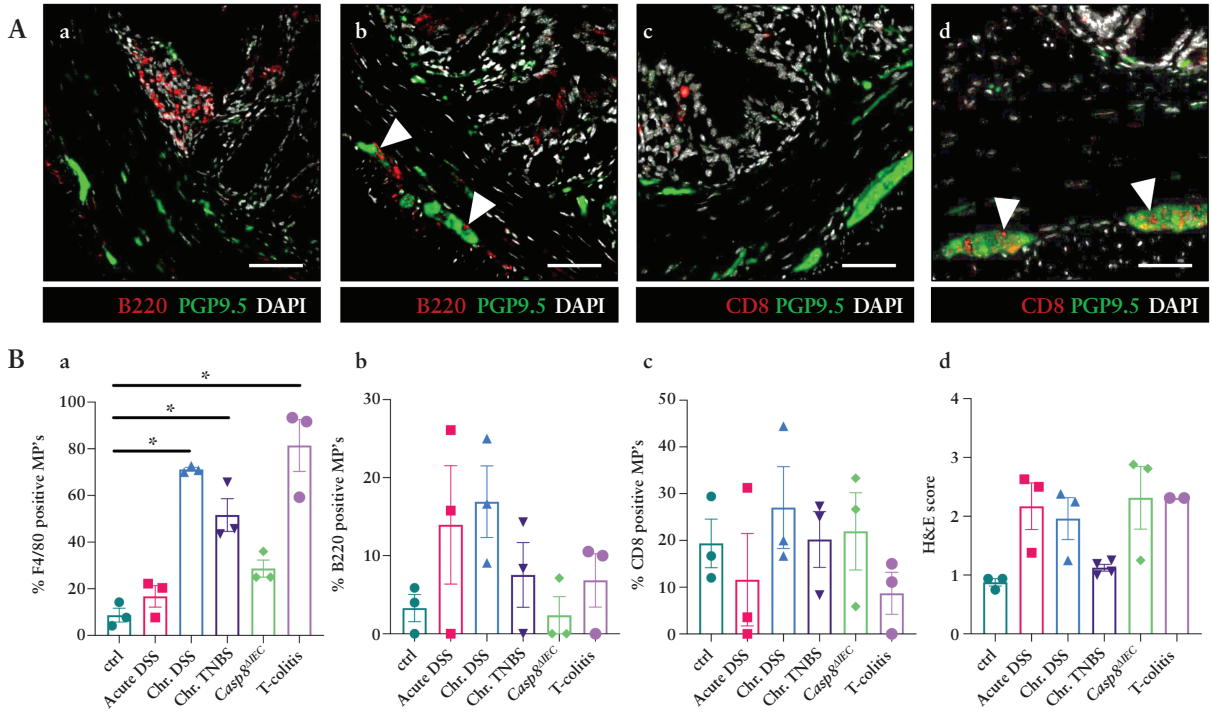

C

	Plexus-dominant infiltration in murine models						Plexus-dom. infiltration IBD		
Cell type/ survival	Murine marker	Acute DSS	Chronic DSS	Chronic TNBS	*Casp8*$^{\Delta IEC}$	Transfer colitis	Human marker	CD	UC
Monocyte/ macrophage	F4/80	↑	↑↑↑***	↑↑**	↑	↑↑↑***	CD68	↑↑**	–
B-cells	B220	↑↑	↑↑	↑	–	↑	CD20	↑*	–
T helper cells	CD4	–	–	↑	–	↑↑	CD4	–	–
Cytotoxic T-cells	CD8	–	↑	–	–	↓	CD8	↑↑**	↑
Apoptosis	Cleaved caspase 3	–	–	–	–	–	Annexin V	–	↑*

Figure 8. Comparison of MP-immune cell infiltration in humans with murine models of intestinal inflammation. [A-a] Control mouse colon. [A-b] Mouse colon in acute DSS-induced colitis with B220$^+$ B cells [red, white arrowheads] located particularly next to PGP9.5$^+$ MP cells [green]. [A-d] Presence of CD8$^+$ T cells [red] within MP in chronic DSS-induced colitis, whereas no CD8$^+$ T cells were observed in MP of the control mouse [A-c]; scale bar, 50 µm. [B-a to B-c] Infiltrations of MPs by immune cells in various murine colitis models [percentage of F4/80$^+$, B220$^+$, CD4$^+$ and CD8$^+$ cells]. F4/80$^+$ cells in close proximity to the plexus are significantly increased in chronic DSS-induced colitis, chronic TNBS-induced colitis and transfer colitis. [B-d] Disease activity in the various mouse models as judged by the histopathology score by Erben *et al.*[33] [C] Summary of MP immune cell compositions. N[acute DSS] = 3, N[chronic DSS] = 3, N[chronic TNBS] = 3, N[chronic TNBS] = 3, N[Transfer-colitis] = 3, N[Casp8ΔIEC] = 3, N[ctrl] = 3. Significance levels were determined using the ANOVA test; *p <0.05; **p <0.01; ***p <0.001]. MP, myenteric plexus; ANOVA, analysis of variance.

difference in MP apoptosis was observed. Taken together, the chronic DSS-induced colitis reflected the findings in human CD-associated colitis most representatively [Figure 8C].

4. Discussion

Abdominal pain is a major complaint of patients suffering from active IBD. Understanding the underlying pathophysiology will allow design of targeted strategies against pain-triggering structures, and thus will contribute to improving pain management. MPs are key structures in transducing pain signals from the mucosa to the CNS.[4] Herein, we have focused on immune cell infiltrations in MPs, revealing disease-specific monocytic and lymphocytic cell populations, and have examined potential consequences on neuronal cell survival and neurotransmitter levels. We included colon tissue from resections of patients who suffered either from UC or Crohn´s colitis. Regarding disease activity of the respective IBD, the patients included had passed a threshold requiring a surgical intervention. Colon wall tissue was examined using haematoxylin and eosin [H&E] staining, conventional IHC as well as IF followed by confocal microscopy. Furthermore, comparisons of human and murine immunostaining were performed to determine which colitis mouse mode reflects best the human immune cell infiltration of MP. This will expand future experimental options in selecting the optimal mouse model in studying IBD-specific changes on the MP level.

4.1. IBD does not affect MP morphology or plexus density

Although to some extent phenotypically different, the IBDs are both elicited by a defective mucosal immune barrier rather than a defect in the outer layers of the gut. However, it is conceivable that the structural integrity of MPs is affected secondary to an intensive infiltration of the gut wall by immune cells. This might result in a reduction of the number of MP ganglia or a size reduction. Contrary to this hypothesis and to some reports of others, we found MPs to be equally distributed and largely of similar size in IBD compared with control colon tissue, using conventional light microscopy.[20] Regarding plexus size, we only found a statistically non-significant tendency to smaller MPs in CD, which is known to regularly display a transmural histopathological distribution.

When comparing these findings with the literature, an age-dependent myenteric cell loss has been observed in the human small intestine[36] and in the colon.[37] Previous works on the ENS in IBD revealed morphological alterations including an irregular network of mostly hypertrophic mucosal nerve fibres and axonal necrosis.[21,38] With respect to MPs, ganglion cell hypertrophy was found, a finding that we were not able to reproduce, and also damage of plexus-associated nerve fibres, which was identified by transmission electron microscopy, a technique not applied in this study.[19,20]

Regarding the mechanisms underlying altered MP integrity in non-congenital intestinal diseases, the loss of myenteric gangliocytes is described to be caused by ganglion cell apoptosis.[39] Similarly, murine dinitrobenzene sulphonic acid [DNBS] colitis causes apoptosis of HuC/D$^+$ neurons.[40] In line with this finding, we detected increased levels of apoptosis in MP gangliocytes in UC but not in CD.

4.2. Disease-specific patterns of infiltrating immune cells in myenteric plexitis

In this study, we have examined the immune cell populations that constitute myenteric plexitis in a relevant number of IBD patients. The most striking differences compared with healthy control individuals were found regarding monocyte and B cell numbers in CD patients. Moreover, T cell populations were found to be shifted as well, thereby disclosing the complexity of the plexitis phenotype in CD and UC.

It is known from murine studies that, upon inflammation, monocytes extravasate from high endothelial venules into the intestinal mucosa to acutely contribute to the early inflammatory response or to differentiate into longer-lived macrophages or DC-like cells.[35] Our study reveals that monocytes also have the potential to significantly infiltrate MP in inflammation, as we have found in CD. This appears to be specific to MP rather than to the whole muscular layer, since a comparably significant infiltration by monocytes was not found in the periganglionic area. This is supported by the recent description of an intraganglionic population of macrophages that penetrate the agrin-based blood-MP barrier in the murine DSS-induced colitis model.[26] Whether such a barrier exists around human MPs, and whether or not IBD affects the integrity of this barrier, needs to be further investigated.

Furthermore, it is well known that monocytes are chemotactically attracted to specific target sites by a set of chemokines, as proven for monocyte chemoattractant protein-1 [MIP1] binding to its CC chemokine receptor type-2 [CCR2] which is expressed on monocytes.[35] It was thus suggestive that expression of the CCR2-ligand MIP1 by enteric gangliocytes—possibly induced in pro-inflammatory conditions—might contribute to monocyte chemoattraction in IBD, as this chemokine is also strongly expressed by CNS neuronal cells.[41] Furthermore, motility dysfunctions elicited by monocytic cells in murine TNBS-induced colitis were shown to be MIP1-dependent.[42] Analogous findings were published for mice infected with the neurotropic herpes simplex virus-1.[43] In line with these findings, we found CCR2 to be strongly expressed by monocytes in the MP but also by other MP cells, suggesting chemotaxis of CCR2-expressing monocytes towards the MP.

Since both IBDs are not regarded to be specifically B cell-mediated, and treatment strategies targeting B cells were found to be unsuccessful in controlling IBD in a phase 2 clinical study,[44] our finding of significantly elevated B cell counts in MPs in CD came with some surprise. In this case however, this highly significant finding was not restricted to the intraganglionic space but was instead replicated in the periganglionic area as well. Thus it could also reflect elevated B cell counts in the muscularis propria in CD as well. Nevertheless, we identified CD20$^+$ B cells directly next to PGP9.5$^+$ myenteric neurons in six patients suffering from CD [Figure 3B']. Considering the function of B cells in an autoimmune context of neuronal damage suggests comparison of this pathology with multiple sclerosis [MS]. However, one major target of the immune reaction in MS is the myelin sheath, contributing to demyelination as the core pathology in MS.[45,46] This is in clear contrast to neurites of ENS gangliocytes being devoid of a myelin sheath. Nevertheless, Rao *et al.* have shown that enteric glia within the MPs express myelin-building proteins proteolipid protein-1 [PLP1], myelin basic protein [MBP], myelin protein zero [MPZ], and 20,30-cyclic nucleotide 30 phosphodiesterase,[47] which might comprise the target of B cells.

With regard to T cells, it is established that certain cell subsets are activated in the context of a defective mucosal barrier, drive the IBD-specific pathology, and therefore are found in increased numbers in the gut lamina propria: Th1-type, IFN-γ-secreting CD4$^+$ T-helper cells, CD4$^+$CD25$^+$ regulatory T cells,[48] and CD8$^+$ T-effector cells.[49] The MP immune cell infiltration we have identified in CD comprised significantly increased periganglionic CD4$^+$ cell counts and a tendency to higher intraganglionic CD4$^+$ cells. Interestingly, CD8$^+$ effector T cells infiltrated MPs in CD and were also found—at least in the periganglionic area—in UC. CD8$^+$ T cells primed to IFN-γ producing Tc1 cells by IL-12 have the potential to lyse target cells by granzyme B and perforin, and thereby elicit direct cytotoxicity to MP neurons.[50] Previously, it was shown that depletion of Tc1 cells was sufficient to prevent murine colitis, implying a crucial role for these cells in colitis induction.[51] In line with this, cytotoxic, granzyme B-secreting CD8$^+$ T cells were found to be increased in surgical Crohn´s resections as well as in the peripheral blood of patients with CD.[52] Since CD8$^+$ T cells were the only immune cell population, and we have specifically identified that in UC-MPs and MPs affected in UC were subject to ganglional cell death, it is tempting to speculate that MP cell death in UC is associated with CD8$^+$ T cell cytotoxicity. Moreover, tissue-resident CD8$^+$ T cells are thought to propagate neuroinflammation in MS.[53] Indeed, in experimental autoimmune encephalomyelitis [EAE], which is a murine model for MS, immunisation of mice

against myelin-derived epitopes led to neuroinflammation caused by CD4+ and CD8+ T cells.[54]

When comparing our T cell findings in MPs with the non-IBD literature, it is worthwhile mentioning that Tornblom *et al*. identified CD3+ T cell infiltrations in MP ganglia in irritable bowel syndrome [IBS] and[55] that De Giorgio *et al*. similarly identified increased T-helper cell counts in MPs of three patients suffering from chronic intestinal pseudo-obstruction [CIPO],[56] thereby documenting that MP-infiltrating T cells also occur in gastrointestinal [GI] motility disorders in which the MP is regarded as a core structure involved in the initiation of disease.

4.3. Expression of neuropeptides and TRP channels in IBD-MPs

For initiation of visceral pain, nociceptors on afferent sensory neurons are mechanically or chemically activated. The peripheral nociceptive information is selectively transmitted via the spinal dorsal horn to the CNS where it is integrated, resulting in pain sensations. Spinal sensory afferent nerves, mostly C-fibres, are characterised by predominant peptidergic transmission as by CGRP or SP. Peripheral projections of afferents innervating the colon include mucosal, muscular, vascular, and mechanically insensitive or silent afferents. Additional to structural differences, the neuronal excitability of the various spinal afferents is regulated by distinct ion channels and receptors as the pro-nociceptive channels TRPA1, TRPV1, TRPV4, and the antinociceptive μ-opioid receptor. During inflammation, the visceral sensitivity provided by afferents can be strongly imbalanced. Variable mediators, including SP, nerve growth factor, and TNF-α, can activate and sensitise receptors on sensory nerves, especially silent afferents. This sensitisation, caused by inflammatory conditions, can lead to an enhanced response to noxious stimuli, resulting in chronic visceral hypersensitivity that is suggested to play a major role in the development of chronic abdominal pain.[57]

In our study, expression of the neurotransmitters CGRP and SP in MP cells was investigated by IHC and revealed an IBD-specific pattern. A higher CGRP expression was found in MP of UC patients. Furthermore, CGRP-positive ganglia were specifically infiltrated by CD68+ monocytes in UC. CGRP is known as a neurotransmitter and neuromodulator relevant for the transmission of pain signals and, at the same time, a transducing factor of the neuroimmune synapse and as such a communicator to various immune cells.[58] Interestingly, it was published that CGRP secretion promotes the development of a regulatory phenotype of TLR4-stimulated macrophages, thereby counteracting a pro-inflammatory action of macrophages.[59] This is in line with data on rats treated with a CGRP antagonist that caused a worsening of TNBS-induced colitis on the one hand. On the other hand, a CGRP knock-out exacerbated murine oxazolone-induced colitis activity. Thus, CGRP expression in UC-MPs spatially associated with CD68+ macrophages might contribute to establishing a more regulatory type of macrophage infiltrate[60,61]

For SP, the second neuropeptide we analysed, expression in MPs was found reduced in CD compared with MP gangliocytes of control colon. This is in line with previous data revealing decreased SP levels in the rectum of patients with CD.[62] However, others demonstrated increased SP in hypervascular lesions of CD.[63,64] Previous studies in murine models of IBD suggested that SP is contributing to the inflammatory process, since SP knock-out mice were protected against oxazolone colitis and an NK1 receptor antagonist also ameliorated activity of DSS-induced colitis.[61,65] In contrast to our finding at the level of MP, Utsumi *et al*. also uncovered that in the mucosa of the inflamed murine colon SP+ nerve fibres increase in number and fibre length and that, in parallel, the receptor for SP [neurokinin-1 receptor] is upregulated mostly in CD11b+ lamina propria macrophages.[65] Interestingly, SP activity might also be modulated by non-gangliocyte MP cells, specifically glial cells, which produce glial cell-derived neurotrophic-factor [GDNF], having an impact on the release of SP.[66]

Our experiments on TRP channels revealed the upregulation of TRPV4 in MPs, specifically in the presence of CD68+ macrophages in both IBDs, which is generally in line with the notion that TRPV4 channels are upregulated in various types of inflammation, including urinary tract, pancreas, and adipose tissue. This, in the past, already has generated the question whether the TRPV4 channel might be a good target for future anti-inflammatory treatments.[67] Furthermore, TRPV4 channels have been identified as important players in the induction of visceral pain/visceral hypersensitivity, which supports the working model that IBD-specific immune cells [macrophages] contribute to pain development.[68,69] Last, and also interesting for our setting, is a recent finding that not only MP neurons but also MP macrophages express TRPV4, thereby having an impact on colon motility via prostaglandin release. In the context of increased TRPV4 in IBD, this offers some explanation for the altered motility in actively inflamed IBD.[70]

4.4. Conclusion

In the present work we have focused on colonic MPs. Results of our study reveal that in both CD and UC, a specific MP inflammatory infiltrate exists, which comprises monocytes, B cells, and CD8+ T cells in CD and CD8+ T cells in UC. These immune cell populations likely contribute to the development of visceral pain and hypersensitivity in IBD and might add to the increased gangliocyte apoptosis that we found in UC. Moreover, we have identified differences in the expression of the pain-relevant neurotransmitters CGRP and SP and the nociceptive cation channel TRPV4. Last, we compared these findings with the most relevant murine models of intestinal inflammation and identified the chronic DSS-induced colitis as the most representative model regarding the study of IBD-associated changes in MP. Further investigation needs to be performed to reach a more detailed insight into underlying mechanisms of the interactions of inflammation, motility, and pain in IBD, which finally can lead to development of new targeted therapeutic options for pain in IBD[67–70].

The data underlying this article are available in the article and in its online Supplementary material.

Funding

CB, JW, MB, MP, BS, AAK, and MS were funded by the Deutsche Forschungsgemeinschaft [DFG, German Research Foundation] – TRR 241 – 375876048 [C03, and B01, B05, C01, Z02, Z03].

Conflict of Interest

The authors have nothing to disclose.

Author Contributions

JJW: concept and design of the study, immunostaining and evaluation of human and murine colon tissue, analysis and

interpretation of data. SM: RT-PCR, imaging, writing of a methods paragraph. AAK: advice on immunostaining of human colon tissue and immunostaining of colitis mouse model colon tissue, analysis and interpretation of data, and revising critically for important intellectual content. AF: evaluation of immunostained human colon tissue. SE: provision of samples and evaluation of immunostained human colon tissue. ES: evaluation and acquisition of patient data. MB: scoring of murine models of intestinal inflammation. RA: concept and design of the study and revising it critically for important intellectual content. CB: concept and design of the study and revising it critically for important intellectual content. BW: provision of samples, acquisition of data. BS: concept and design of the study and revising it critically for important intellectual content. JVP: help with immunostaining of colitis mouse model colon tissue and revising critically for important intellectual content. MSP: concept and design of the study and revising it critically for important intellectual content. MS: concept and design of the study, acquisition of data, analysis, interpretation of data, and revising critically for important intellectual content.

Acknowledgements

We thank Claudia Günther, Claudia Heldt, Simone Spieckermann, Hedwig Lammert, Lena Schödel, Verena Moos, and Jörg Scheffel for technical help.

Supplementary Data

Supplementary data are available at *ECCO-JCC* online.

References

1. Martini E, Krug SM, Siegmund B, Neurath MF, Becker C. Mend your fences: The epithelial barrier and its relationship with mucosal immunity in inflammatory bowel disease. *Cell Mol Gastroenterol Hepatol* 2017;**4**:33–46.
2. Chang JT. Pathophysiology of inflammatory bowel diseases. *N Engl J Med* 2020;**383**:2652–64.
3. Srinath A, Young E, Szigethy E. Pain management in patients with inflammatory bowel disease: Translational approaches from bench to bedside. *Inflamm Bowel Dis* 2014;**20**:2433–49.
4. Furness JB. The enteric nervous system and neurogastroenterology. *Nat Rev Gastroenterol Hepatol* 2012;**9**:286–94.
5. Yoo BB, Mazmanian SK. The enteric network: Interactions between the immune and nervous systems of the gut. *Immunity* 2017;**46**:910–26.
6. Smith-Edwards KM, Najjar SA, Edwards BS, Howard MJ, Albers KM, Davis BM. Extrinsic primary afferent neurons link visceral pain to colon motility through a spinal reflex in mice. *Gastroenterology* 2019;**157**:522–36.e2.
7. Spencer NJ, Zagorodnyuk V, Brookes SJ, Hibberd T. Spinal afferent nerve endings in visceral organs: Recent advances. *Am J Physiol Gastrointest Liver Physiol* 2016;**311**:G1056–63.
8. Chow BY, Han X, Dobry AS, *et al*. High-performance genetically targetable optical neural silencing by light-driven proton pumps. *Nature* 2010;**463**:98–102.
9. Najjar SA, Ejoh LL, Loeza-Alcocer E, *et al*. Optogenetic inhibition of the colon epithelium reduces hypersensitivity in a mouse model of inflammatory bowel disease. *Pain* 2021;**162**:1126–34.
10. Song ZM, Brookes SJ, Costa M. Identification of myenteric neurons which project to the mucosa of the guinea-pig small intestine. *Neurosci Lett* 1991;**129**:294–8.
11. Brierley SM, Linden DR. Neuroplasticity and dysfunction after gastrointestinal inflammation. *Nat Rev Gastroenterol Hepatol* 2014;**11**:611–27.
12. Chahl LA. Antidromic vasodilatation and neurogenic inflammation. *Pharmacol Ther* 1988;**37**:275–300.
13. Holzer P. Local effector functions of capsaicin-sensitive sensory nerve endings: Involvement of tachykinins, calcitonin gene-related peptide and other neuropeptides. *Neuroscience* 1988;**24**:739–68.
14. Maggi CA. Tachykinins and calcitonin gene-related peptide [cgrp] as co-transmitters released from peripheral endings of sensory nerves. *Prog Neurobiol* 1995;**45**:1–98.
15. Shimizu Y, Matsuyama H, Shiina T, Takewaki T, Furness JB. Tachykinins and their functions in the gastrointestinal tract. *Cell Mol Life Sci* 2008;**65**:295–311.
16. Chandrasekharan B, Nezami BG, Srinivasan S. Emerging neuropeptide targets in inflammation: Npy and vip. *Am J Physiol Gastrointest Liver Physiol* 2013;**304**:G949–57.
17. Bednarska O, Walter SA, Casado-Bedmar M, *et al*. Vasoactive intestinal polypeptide and mast cells regulate increased passage of colonic bacteria in patients with irritable bowel syndrome. *Gastroenterology* 2017;**153**:948–60.e3.
18. Seo S, Miyake H, Alganabi M, *et al*. Vasoactive intestinal peptide decreases inflammation and tight junction disruption in experimental necrotizing enterocolitis. *J Pediatr Surg* 2019;**54**:2520–3.
19. Collins SM, Van Assche G, Hogaboam C. Alterations in enteric nerve and smooth-muscle function in inflammatory bowel diseases. *Inflamm Bowel Dis* 1997;**3**:38–48.
20. Storsteen KA, Kernohan JW, Bargen JA. The myenteric plexus in chronic ulcerative colitis. *Surg Gynecol Obstet* 1953;**97**:335–43.
21. Dvorak AM, Silen W. Differentiation between crohn's disease and other inflammatory conditions by electron microscopy. *Ann Surg* 1985;**201**:53–63.
22. Belai A, Boulos PB, Robson T, Burnstock G. Neurochemical coding in the small intestine of patients with crohn's disease. *Gut* 1997;**40**:767–74.
23. Schneider J, Jehle EC, Starlinger MJ, *et al*. Neurotransmitter coding of enteric neurones in the submucous plexus is changed in non-inflamed rectum of patients with crohn's disease. *Neurogastroenterol Motil* 2001;**13**:255–64.
24. Villanacci V, Bassotti G, Nascimbeni R, *et al*. Enteric nervous system abnormalities in inflammatory bowel diseases. *Neurogastroenterol Motil* 2008;**20**:1009–16.
25. Domoto R, Sekiguchi F, Tsubota M, Kawabata A. Macrophage as a peripheral pain regulator. *Cells* 2021;**10**:1881.
26. Dora D, Ferenczi S, Stavely R, *et al*. Evidence of a myenteric plexus barrier and its macrophage-dependent degradation during murine colitis: Implications in enteric neuroinflammation. *Cell Mol Gastroenterol Hepatol* 2021;**12**:1617–41.
27. De Schepper S, Verheijden S, Aguilera-Lizarraga J, *et al*. Self-maintaining gut macrophages are essential for intestinal homeostasis. *Cell* 2018;**175**:400–15.e13.
28. Pannell M, Labuz D, Celik MO, *et al*. Adoptive transfer of m2 macrophages reduces neuropathic pain via opioid peptides. *J Neuroinflammation* 2016;**13**:262.
29. Schumann M, Gunzel D, Buergel N, *et al*. Cell polarity-determining proteins par-3 and pp-1 are involved in epithelial tight junction defects in coeliac disease. *Gut* 2012;**61**:220–8.
30. Schumann M, Richter JF, Wedell I, *et al*. Mechanisms of epithelial translocation of the alpha[2]-gliadin-33mer in coeliac sprue. *Gut* 2008;**57**:747–54.
31. Wirtz S, Popp V, Kindermann M, *et al*. Chemically induced mouse models of acute and chronic intestinal inflammation. *Nat Protoc* 2017;**12**:1295–309.
32. Eri R, McGuckin MA, Wadley R. T cell transfer model of colitis: a great tool to assess the contribution of t cells in chronic intestinal inflammation. *Methods Mol Biol* 2012;**844**:261–75.
33. Erben U, Loddenkemper C, Doerfel K, *et al*. A guide to histomorphological evaluation of intestinal inflammation in mouse models. *Int J Clin Exp Pathol* 2014;**7**:4557–76.
34. Stolzer I, Schickedanz L, Chiriac MT, *et al*. Stat1 coordinates intestinal epithelial cell death during gastrointestinal infection upstream of caspase-8. *Mucosal Immunol* 2022;**15**:130–42.

35. Trzebanski S, Jung S. Plasticity of monocyte development and monocyte fates. *Immunol Lett* 2020;**227**:66–78.
36. de Souza RR, Moratelli HB, Borges N, Liberti EA. Age-induced nerve cell loss in the myenteric plexus of the small intestine in man. *Gerontology* 1993;**39**:183–8.
37. Gomes OA, de Souza RR, Liberti EA. A preliminary investigation of the effects of aging on the nerve cell number in the myenteric ganglia of the human colon. *Gerontology* 1997;**43**:210–7.
38. Geboes K, Collins S. Structural abnormalities of the nervous system in crohn's disease and ulcerative colitis. *Neurogastroenterol Motil* 1998;**10**:189–202.
39. Zhou Y, Yang J, Watkins DJ, *et al*. Enteric nervous system abnormalities are present in human necrotizing enterocolitis: potential neurotransplantation therapy. *Stem Cell Res Ther* 2013;**4**:157.
40. Boyer L, Ghoreishi M, Templeman V, *et al*. Myenteric plexus injury and apoptosis in experimental colitis. *Auton Neurosci* 2005;**117**:41–53.
41. Banisadr G, Gosselin RD, Mechighel P, Kitabgi P, Rostene W, Parsadaniantz SM. Highly regionalized neuronal expression of monocyte chemoattractant protein-1 [mcp-1/ccl2] in rat brain: evidence for its colocalization with neurotransmitters and neuropeptides. *J Comp Neurol* 2005;**489**:275–92.
42. Hori M, Nobe H, Horiguchi K, Ozaki H. Mcp-1 targeting inhibits muscularis macrophage recruitment and intestinal smooth muscle dysfunction in colonic inflammation. *Am J Physiol Cell Physiol* 2008;**294**:C391–401.
43. Brun P, Qesari M, Marconi PC, *et al*. Herpes simplex virus type 1 infects enteric neurons and triggers gut dysfunction via macrophage recruitment. *Front Cell Infect Microbiol* 2018;**8**:74.
44. Leiper K, Martin K, Ellis A, *et al*. Randomised placebo-controlled trial of rituximab [anti-cd20] in active ulcerative colitis. *Gut* 2011;**60**:1520–6.
45. Piddlesden SJ, Lassmann H, Zimprich F, Morgan BP, Linington C. The demyelinating potential of antibodies to myelin oligodendrocyte glycoprotein is related to their ability to fix complement. *Am J Pathol* 1993;**143**:555–64.
46. Elliott C, Lindner M, Arthur A, *et al*. Functional identification of pathogenic autoantibody responses in patients with multiple sclerosis. *Brain* 2012;**135**:1819–33.
47. Rao M, Nelms BD, Dong L, *et al*. Enteric glia express proteolipid protein 1 and are a transcriptionally unique population of glia in the mammalian nervous system. *Glia* 2015;**63**:2040–57.
48. Zenewicz LA, Antov A, Flavell RA. Cd4 t cell differentiation and inflammatory bowel disease. *Trends Mol Med* 2009;**15**:199–207.
49. Casalegno Garduno R, Dabritz J. New insights on cd8[+] t cells in inflammatory bowel disease and therapeutic approaches. *Front Immunol* 2021;**12**:738762.
50. St Paul M, Ohashi PS. The roles of cd8[+] t cell subsets in antitumor immunity. *Trends Cell Biol* 2020;**30**:695–704.
51. Nancey S, Holvoet S, Graber I, *et al*. Cd8+ cytotoxic t cells induce relapsing colitis in normal mice. *Gastroenterology* 2006;**131**:485–96.
52. Boschetti G, Nancey S, Moussata D, *et al*. Enrichment of circulating and mucosal cytotoxic cd8+ t cells is associated with postoperative endoscopic recurrence in patients with crohn's disease. *J Crohns Colitis* 2016;**10**:338–45.
53. Lassmann H. Pathogenic mechanisms associated with different clinical courses of multiple sclerosis. *Front Immunol* 2018;**9**:3116.
54. Brandao WN, De Oliveira MG, Andreoni RT, Nakaya H, Farias AS, Peron JPS. Neuroinflammation at single cell level: what is new? *J Leukoc Biol* 2020;**108**:1129–37.
55. Tornblom H, Lindberg G, Nyberg B, Veress B. Full-thickness biopsy of the jejunum reveals inflammation and enteric neuropathy in irritable bowel syndrome. *Gastroenterology* 2002;**123**:1972–9.
56. De Giorgio R, Barbara G, Stanghellini V, *et al*. Clinical and morphofunctional features of idiopathic myenteric ganglionitis underlying severe intestinal motor dysfunction: a study of three cases. *Am J Gastroenterol* 2002;**97**:2454–9.
57. Grundy L, Erickson A, Brierley SM. Visceral pain. *Annu Rev Physiol* 2019;**81**:261–84.
58. Assas BM, Pennock JI, Miyan JA. Calcitonin gene-related peptide is a key neurotransmitter in the neuro-immune axis. *Front Neurosci* 2014;**8**:23.
59. Baliu-Piqué M, Jusek G, Holzmann B. Neuroimmunological communication via CGRP promotes the development of a regulatory phenotype in TLR4-stimulated macrophages. *Eur J Immunol* 2014;**44**:3708–16.
60. Reinshagen M, Flamig G, Ernst S, *et al*. Calcitonin gene-related peptide mediates the protective effect of sensory nerves in a model of colonic injury. *J Pharmacol Exp Ther* 1998;**286**:657–61.
61. Engel MA, Khalil M, Siklosi N, *et al*. Opposite effects of substance p and calcitonin gene-related peptide in oxazolone colitis. *Dig Liver Dis* 2012;**44**:24–9.
62. Bernstein CN, Robert ME, Eysselein VE. Rectal substance p concentrations are increased in ulcerative colitis but not in crohn's disease. *Am J Gastroenterol* 1993;**88**:908–13.
63. Mazumdar S, Das KM. Immunocytochemical localization of vasoactive intestinal peptide and substance p in the colon from normal subjects and patients with inflammatory bowel disease. *Am J Gastroenterol* 1992;**87**:176–81.
64. Kimura M, Kishida R, Abe T, Goris RC, Kawai S. Nerve fibers immunoreactive for substance p and calcitonin gene-related peptide in the cervical spinal ventral roots of the mouse. *Cell Tissue Res* 1994;**277**:273–8.
65. Utsumi D, Matsumoto K, Amagase K, Horie S, Kato S. 5-ht3 receptors promote colonic inflammation via activation of substance p/neurokinin-1 receptors in dextran sulphate sodium-induced murine colitis. *Br J Pharmacol* 2016;**173**:1835–49.
66. Gianino S, Grider JR, Cresswell J, Enomoto H, Heuckeroth RO. Gdnf availability determines enteric neuron number by controlling precursor proliferation. *Development* 2003;**130**:2187–98.
67. Vergnolle N. Trpv4: new therapeutic target for inflammatory bowel diseases. *Biochem Pharmacol* 2014;**89**:157–61.
68. Cenac N, Altier C, Motta JP, *et al*. Potentiation of trpv4 signalling by histamine and serotonin: an important mechanism for visceral hypersensitivity. *Gut* 2010;**59**:481–8.
69. Cenac N, Altier C, Chapman K, Liedtke W, Zamponi G, Vergnolle N. Transient receptor potential vanilloid-4 has a major role in visceral hypersensitivity symptoms. *Gastroenterology* 2008;**135**:937–46, 946.e1.
70. Luo J, Qian A, Oetjen LK, *et al*. Trpv4 channel signaling in macrophages promotes gastrointestinal motility via direct effects on smooth muscle cells. *Immunity* 2018;**49**:107–19.e4.